

Document downloaded from:

<http://hdl.handle.net/10251/183952>

This paper must be cited as:

Giraldo-Guzmán, J.; Kotas, M.; Castells, F.; Contreras-Ortiz, SH.; Urina-Triana, M. (2021). Estimation of PQ distance dispersion for atrial fibrillation detection. *Computer Methods and Programs in Biomedicine*. 208:1-12. <https://doi.org/10.1016/j.cmpb.2021.106167>



The final publication is available at

<https://doi.org/10.1016/j.cmpb.2021.106167>

Copyright Elsevier

Additional Information

Estimation of PQ distance dispersion for atrial fibrillation detection ^{*}

Elsevier¹

Radarweg 29, Amsterdam

Jader Giraldo-Guzmán^{a,*}, Marian Kotas^b, Francisco Castells^c, Sonia H. Contreras-Ortiz^a, Miguel Urina-Triana^d

^aFaculty of engineering, Universidad Tecnológica de Bolívar
Km 1 Via Turbaco, Cartagena de Indias, 130010, Colombia

^bDepartment of Cybernetics, Nanotechnology and Data Processing, Silesian University of Technology, Akademicka 16, Gliwice, 44-100, Poland

^cInstituto ITACA, Universitat Politècnica de València (UPV), Spain

^dFaculty of health sciences, Universidad Simón Bolívar
Carrera 54 # 64 - 222, Barranquilla, 1086, Colombia

Abstract

Background and objective: Atrial fibrillation (AF) is the most common cardiac arrhythmia in the world. It is associated with significantly increased morbidity and mortality. Diagnosis of the disease can be based on the analysis of the electrical atrial activity, on quantification of the heart rate irregularity or on a mixture of the both approaches. Since the amplitude of the atrial waves is small, their analysis can lead to false results. On the other hand, the heart rate based analysis usually leads to many unnecessary warnings. Therefore, our goal is to develop a new method for effective AF detection based on the analysis of the electrical atrial waves.

Methods: The proposed method employs the fact that there is a lack of repeatable P waves preceding QRS complexes during AF. We apply the operation of spatio-temporal filtering (STF) to magnify and detect the prominent spatio-temporal patterns (STP) within the P waves in multi-channel ECG recordings.

^{*}Fully documented templates are available in the elsarticle package on CTAN.

^{*}Corresponding author

Email address: jgiraldo@utbvirtual.edu.co (Jader Giraldo-Guzmán)

¹Since 1880.

Later we measure their distances (PQ) to the succeeding QRS complexes, and we estimate dispersion of the obtained PQ series. For signals with normal sinus rhythm, this dispersion is usually very low, and contrary, for AF it is much raised. This allows for effective discrimination of this cardiologic disorder.

Results: Tested on an ECG database consisting of AF cases, normal rhythm cases and cases with normal rhythm restored by the use of cardioversion, the method proposed allowed for AF detection with the accuracy of 98.75% on the basis of both 8-channel and 2-channel signals of 12 s length. When the signals length was decreased to 6 s, the accuracy varied in the range of 95% – 97.5% depending on the number of channels and the dispersion measure applied.

Conclusions: Our approach allows for high accuracy of atrial fibrillation detection using the analysis of electrical atrial activity. The method can be applied to an early detection of the disease and can advantageously be used to decrease the number of false warnings in systems based on the analysis of the heart rate.

Keywords: ECG processing, atrial fibrillation, PQ dispersion, spatio-temporal filtering, spatio-temporal patterns

2010 MSC: 00-01, 99-00

1. Introduction

Stroke is the third cause of death in the world [1], being a major problem associated to atrial fibrillation (AF), the most common cardiac arrhythmia, as it increases up to 5 times the probability of suffering a stroke [2]. AF is
5 caused by irregular electrical activations of the atria, which in turn causes an irregular ventricular pace. From the ECG, it can be diagnosed from irregular RR intervals and the presence of a continuous and time-varying atrial fibrillatory signal instead of P-waves.

Due to the importance of early detection, in the last years different ap-
10 proaches for automated detection of AF have been proposed, which can be mainly divided in three groups: analysis of the periodicity of the heart rate,

characterization of the atrial activity and hybrid methods involving both strategies [3]. Methods based on the heart rate focus on the analysis of the RR interval and the quantification of its variability, using e.g.: standard deviation, turning
15 point ratio, histogram, Poincaré plots, entropy or spectral analysis of the RR series, among others [4, 5, 6, 7]. In some publications, the approach based on machine learning is proposed to perform classification using the features extracted from the RR series [8], [9]. The main limitations of these methods are related to their specificity, specially in short recordings, as variations of the RR
20 interval are not specific to AF.

Regarding the characterization of the atrial activity, some methods perform spectral analysis, as the atrial fibrillatory wave present distinctive spectral features with respect to the P-wave [10]. These methods require a previous step for QRS-T cancellation [11, 12]. On the other hand, methods aiming to detect the
25 lack of P-waves have been recently proposed, such as Gaussian mixture models trained from morphological and statistical features of the atrial signal [13]. In general, methods based on the characterization of the atrial activity also present inherent limitations due to the low amplitude of the atrial signal.

Hybrid methods combine information from both strategies, extracting frequency and time domain features to characterize the RR series as well as the
30 atrial signal, which further on, can be input to various machine learning approaches for classification [14],[15], [16]. Hybrid methods offer higher performance, and any improvement of the previous methods can be integrated into them. In some of the relatively recent publications, the use of convolutional
35 neural networks (CNN) is proposed for extraction of the both types of information (related with the atrial activity and the ventricular rhythm) without the necessity of advanced signal processing [17], [18],[19],[20]. In spite of the great progress in the development of approaches to AF detection, they are not fully satisfactory yet. The main problem is still with the limited accuracy in
40 the diagnostics of AF in large groups of population, as they produce numerous false positives which have to be verified by cardiologists [21]. Thus, due to the implications of massive screenings with the increase of workload for cardiology

units, this operation may not be cost-effective yet [22].

This work deals with developing a robust and reliable method regarding
45 the second strategy mentioned above and, more specifically, with the detection
of presence/absence of P-waves. The proposed method performs a backward
search within segments preceding QRS complexes to detect either P waves or
some false peaks when the wave does not exist. It is carried out by applying
a spatio-temporal filter [23] where candidate PQ distances are determined and
50 their dispersion assessed. These measures are used to detect the presence of
P-waves and classify the recording as AF in case of P-wave absence.

The paper is organized as follows. Next section describes the materials and
methods. Subsequently, the results are presented. Then, our main findings are
thoroughly discussed before concluding the paper with final remarks.

55 **2. Materials and Methods**

2.1. Multilead ECG database

Eighty ECG recordings were used in our study. Among them, 40 continuous
ECGs from AF patients were registered during an electrical cardioversion (ECV)
using a Prucka 12-lead ECG system. For all patients, excerpts of 12 s were
60 extracted before the electrical shock, which were included in the AF group.
Whenever ECV was successful and ECG data were available (which occurred
in 12 patients), excerpts of 12 s following successful ECV were included in the
normal sinus rhythm (NSR) group (see figure 1. More details about this dataset
can be found in [24]. The NSR group was completed by including 28 ECGs from
65 the PTB Diagnostic ECG Database from Physionet [25]. All recordings were
digitized at a sampling rate of 1 kHz and 16-bit resolution.

2.2. Spatio-temporal filtering

The operation of spatio-temporal filtering (STF) can be applied to multi-
70 channel recordings to enhance a weak desired signal of repeatable morphology

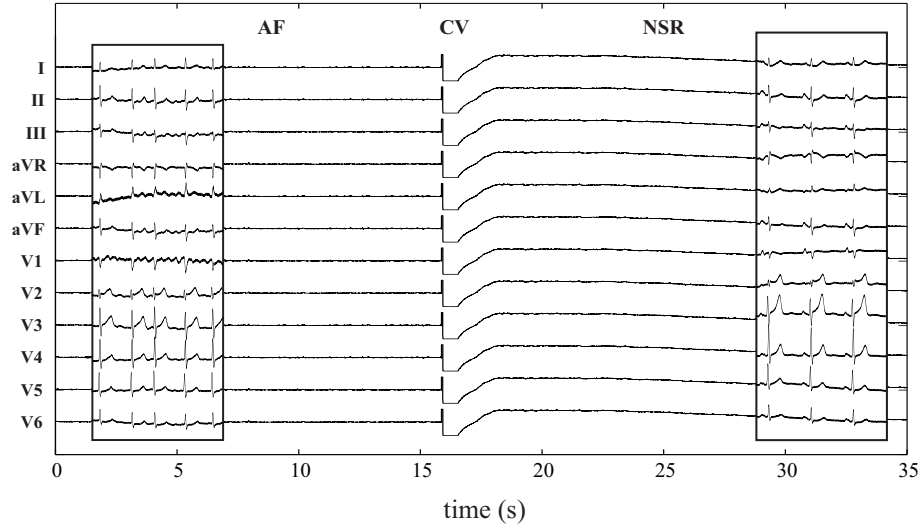


Figure 1: Continuous ECG recording during electrical cardioversion. Previous to the shock, the patient is in AF. During the electrical shock, the amplitude of the signal reaches the full scale of the Analog-to-Digital Converter, hence clipping the signal. If ECV was successful, the cardiac rhythm is converted to NSR.

embedded in high energy noise. Lets denote the m -channel signal as vector $\mathbf{x}(k) = [x_1(k), x_2(k), \dots, x_m(k)]^T$, where k is a time index. To express STF, we form an extended spatio-temporal signal representation [23]:

$$\mathbf{x}^{(k)} = \begin{bmatrix} x_1(k - J\tau) \\ \dots \\ x_m(k - J\tau) \\ x_1(k - (J - 1)\tau) \\ \dots \\ x_m(k - (J - 1)\tau) \\ \dots \\ x_1(k + J\tau) \\ \dots \\ x_m(k + J\tau) \end{bmatrix} \quad (1)$$

containing $2J + 1$ time samples from m channels available (the length of vector

⁷⁵ $\mathbf{x}^{(k)}$ is $p = (2J + 1)m$.

The filtering operation can be expressed as

$$y(k) = \mathbf{h}^T \mathbf{x}^{(k)} \quad (2)$$

with \mathbf{h} being a p -length STF template. To determine this template, we can specify the filter operation by providing a set of spatio-temporal vectors that should be magnified and a set of vectors that should be suppressed. Lets denote as

$$\Gamma_m = \{k_i \mid i = 1, 2, \dots, I_m\} \quad (3)$$

the set of time indices of the vectors to be magnified, and similarly as

$$\Gamma_s = \{k_i \mid i = 1, 2, \dots, I_s\} \quad (4)$$

the corresponding set related with the vectors to be suppressed.

The filter should maximize energy of the responses to vectors $\mathbf{x}^{(k)}$ indicated by Γ_m ($k \in \Gamma_m$) and minimize energy of the responses to those indicated by Γ_s . When the vectors to be magnified contain the repeatable desired component plus independent noise, red the latter can be reduced by averaging:

$$\bar{\mathbf{x}} = \frac{1}{|\Gamma_m|} \sum_{k \in \Gamma_m} \mathbf{x}^{(k)} \quad (5)$$

where $|\Gamma|$ denotes cardinality of Γ .

Then we can define an objective function Q whose maximization will allow to find the proper filter template \mathbf{h} :

$$Q(\mathbf{h}) = \frac{(\mathbf{h}^T \bar{\mathbf{x}})^2}{\frac{1}{|\Gamma_s|} \sum_{k \in \Gamma_s} (\mathbf{h}^T \mathbf{x}^{(k)})^2} = \frac{\mathbf{h}^T \bar{\mathbf{x}} \bar{\mathbf{x}}^T \mathbf{h}}{\mathbf{h}^T \mathbf{C}_s \mathbf{h}} \quad (6)$$

where $\mathbf{C}_s = \sum_{k \in \Gamma_s} \mathbf{x}^{(k)} \mathbf{x}^{(k)T}$.

Maximization of (6) leads to the well-known formula:

$$\mathbf{h} = \mathbf{C}_s^{-1} \bar{\mathbf{x}} \quad (7)$$

which is widely applied for calculation of generalized matched filters (GMF) [26] or common spatial patterns [27],[28]. Similarly like GMF, the STF responds ⁸⁰ with positive peaks to the occurrences of the repeatable desired pattern in the processed signals.

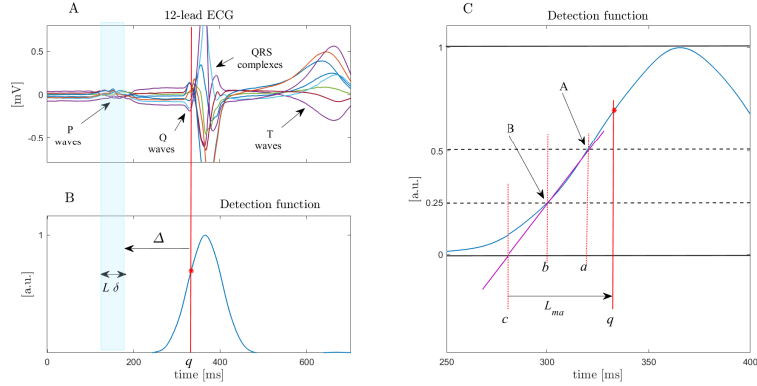


Figure 2: Detection of QRS onsets: A) the processed signal channels, plotted on each other, B) the formed detection function, C) stages of the detection function analysis, leading to the determination of an approximate position q of the Q wave. The position detected allows to establish the segment that should contain the P wave (presented using the blue rectangle). Detailed description of the respective variables, in the text.

2.3. System for atrial fibrillation detection

The system objective is to discriminate between NSR and AF from the presence or absence of P-waves, respectively. As occurs in NSR, regular P-waves precede the ventricular response. Such a state is characterized by a low dispersion of the PQ interval. As this is no longer occurring in AF, the estimation of this dispersion is proposed as the core of the system.

2.3.1. Signal preprocessing and QRS onsets detection

The preprocessing steps involve baseline wander suppression and powerline interference cancellation. Then we perform QRS complexes detection using a multi-channel extension of the Pan-Tompkins algorithm [29]. The filters developed are applied to all channels separately; subsequently, the enhanced signals undergo squaring and addition to form a single-channel one. This signal is finally smoothed by a double sequential application of a moving average (MA) filter [30], [31].

According to this, a QRS detection function is formed (see Fig.2.B), which is employed to estimate the QRS onset, i.e. the Q-wave. Assuming that the height

of the detection function peak equals 1, we search for points A and B, where the
 100 detection function crosses the values of 0.5 and 0.25 and thus, providing time
 instants a and b , respectively (Fig.2.C). From A and B, we define a straight line
 that, at its intersection with the x axis (which occurs at time instant $c = 2b - a$)
 can be estimated as the beginning of the QRS complex. Since, however, the
 detection function peak is widened by the applied moving average, the filter
 105 length L_{ma} must be added ($q = c + L_{ma}$) to compensate for this effect.

After processing a signal containing I_{QRS} QRS complexes, we form a set of
 their onsets ($\Theta = \{q_i, i = 1, 2, \dots, I_{QRS}\}$). They are used to limit the search
 for the P-waves and calculate the PQ intervals variability.

2.3.2. Spatio-temporal filtering for patterns detection within P-waves: the learn- 110 ing phase

The STF learning phase, i.e. determination of the STF coefficients (vector
 \mathbf{h}), is realized for each patient individually, the necessary number of times,
 according to the following procedure.

Since it is the dispersion of the PQ interval that is to be evaluated, the exact
 115 instants of P-wave onset or offset are not required. What is needed instead,
 is the position of some prominent and more easily detectable signal spatio-
 temporal pattern (STP) within this wave. Hence, the dispersion of its distances
 to the succeeding Q waves can be equally regarded as the estimation of the PQ
 dispersion.

To this end, using set Θ of QRS onsets, we determine a family of sets:
 $\Gamma^l, l = 0, 1, \dots, L$, indicating $L + 1$ different assumed positions (within each
 ECG beat) of the searched STPs:

$$\Gamma^l = \{k = q - \Delta - l \cdot \delta \mid q \in \Theta\}, l = 0, 1, 2, \dots, L, \quad (8)$$

120 where Δ is the minimal distance between STP and the succeeding QRS com-
 plexes, and $\Delta + L \cdot \delta$ is the maximal distance assumed (see Fig.2). In advance,
 we will call these distances as the assumed PQ distances.

For each Γ^l , we create a separate STF filter. To achieve it, we must specify

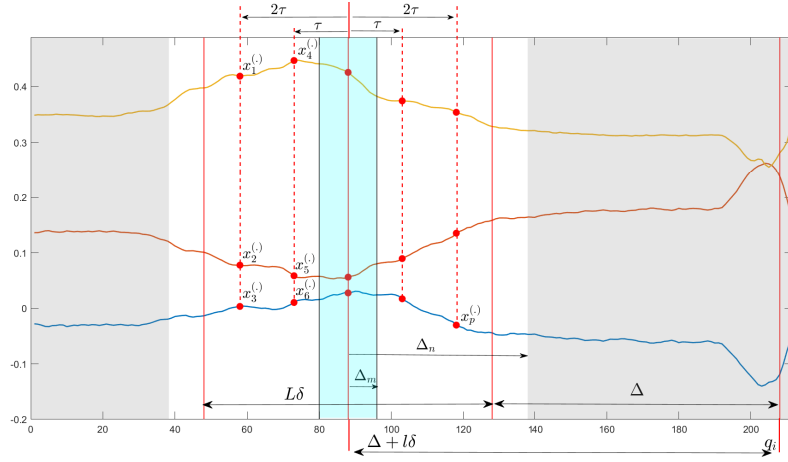


Figure 3: Illustration of the role of the STF learning phase parameters: Δ , δ , L , Δ_m , Δ_n (q_i is the detected position of the i th Q wave). $\Delta + l\delta$, $l = 0, 1, \dots, L$ are the assumed PQ distances; for a given value of l the i th searched spatio-temporal pattern is selected: $\mathbf{x}^{(q_i - \Delta - l\delta)}$, whose entries are marked by red points distributed at the assumed distances around the time index considered; see definition (1). To calculate the STF, the neighboring vectors whose time indices belong to the blue segment (and are limited by Δ_m) are magnified, and those associated with the darkened segments are suppressed (the white segments limited by Δ_n are neglected). The 3-channel signal used for this illustration is vertically separated for better visibility.

a set of spatio-temporal vectors to be magnified (Γ_m^l) and suppressed (Γ_s^l), respectively. Regarding (Γ_m^l), and for each l , we define

$$\Gamma_m^l = \bigcup_{k \in \Gamma^l} \{k' \mid |k' - k| \leq \Delta_m\}. \quad (9)$$

which is a union of sets related with the respective ECG beats, each set comprising $2\Delta_m + 1$ time indices of the vectors to be magnified, surrounding the assumed position of the STP searched (see the illustration in Fig.3). The goal is to magnify the prominent STPs from the P-waves while suppressing the other parts of ECG beats. Since the peaks formed by the filter cannot be extremely sharp and narrow, we neglect the vectors that are close to those indicated by Γ^l

and put the rest to Γ_s^l :

$$\Gamma_s^l = \Gamma - \bigcup_{k \in \Gamma^l} \{k' \mid |k' - k| \leq \Delta_n\}. \quad (10)$$

130 where Γ is the set of all time indices for which spatio-temporal vectors were constructed, $2\Delta_n + 1$ is the number of vectors neglected (not suppressed by STF) within each ECG beat. The role of the respective parameters introduced is explained in Fig. 3.

2.3.3. STF output interpretation

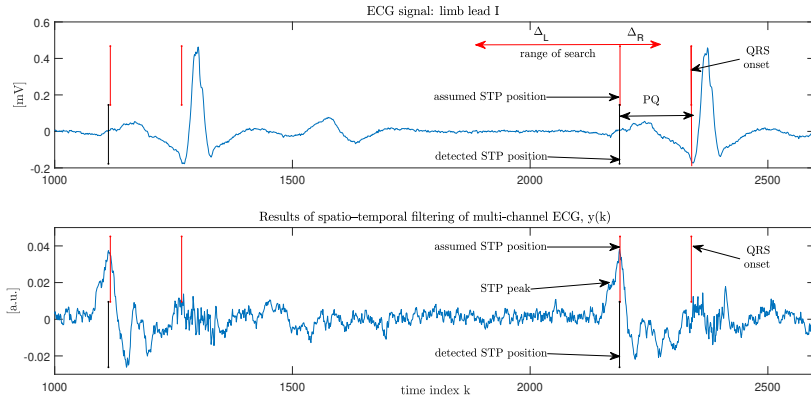


Figure 4: Analysis of the results of STF filtering for STPs detection within P waves. Red vertical lines indicate either QRS onsets or the assumed STP positions. Black vertical lines indicate the positions detected. The range of the search for STP is bounded by the red double sided arrow. The difference between the detected STP position and the QRS onset is regarded as the PQ interval.

135 Within a signal produced by an STF filter, we search for the maxima located near the assumed positions of the patterns magnified. The range of the search is illustrated in Fig.4 using the red double sided arrow (in the experimental section, we assume $\Delta_L = 300$ ms and $\Delta_R = 100$ ms, with the latter parameter much smaller to avoid detection of QRS complexes).

140 After finding the maxima, we calculate their distances to the succeeding QRS complexes. This way for each $\Gamma^l, l = 0, 1, \dots, L$ (and the corresponding

STF filter developed), we obtain an individual PQ series.

2.3.4. PQ dispersion assessment

For each of the $L+1$ PQ series determined, we calculate the chosen measures
145 of dispersion. Since these measures depend not only on the true PQ dispersion
but also on the errors of the border values determination, the smallest among
the $L+1$ values obtained (for each dispersion measure applied) can be regarded
as the best estimate of the true one.

Six dispersion measures have been applied: standard deviation (STD), in-
150 terquartile range (IQR), range (RNG), coefficient of variation (CV), index of
dispersion (ID) and median of absolute deviation (MAD) [32].

2.3.5. Parameters of the system

After some preliminary considerations and experiments, we set the following
values of the respective parameters:

- 155 • $\Delta = 150$ ms and $\delta = 5$ ms, used in (8);
- $\Delta_n = 50$, used in (10);
- $\Delta_L = 300$ ms and $\Delta_R = 100$ ms, illustrated in Fig.4;
- $\tau = 4$; see (1);
- $J = 4$ for 8-channel STF and $J = 15$ for 2-channel STF; see (1);
- 160 • $\Delta_m = 15$ for 8-channel STF and $\Delta_m = 5$ for 2-channel STF; see (10).

The most important parameter J decides on STF length ($2J\tau$), i.e. mostly
on the temporal information exploited by the filter. For 8-channel signals,
the searched spatio-temporal patterns contain significant spatial information,
and therefore J was set to a small value. By contrast, for 2-channel signals,
165 the searched STPs contain rather limited spatial information, and much higher
value had to be chosen, resulting in STF length of $2J\tau=120$ ms, covering ap-
proximately the P-wave.

2.3.6. Selection of independent channels

As it has been described, the experimental database contains 12s excerpts
170 of 12-lead ECG recordings. The standard 12-lead ECG contains 6 limb and 6
precordial leads. Among the limb leads, there are only 2 linearly independent
ones. Therefore, only 8 linearly independent channels are available and, if only
the three electrodes of the limb leads were used, 2 independent channels only.
Using channels that are linear combinations of the other ones does not introduce
175 new information and does not improve the proposed method operation. Con-
sequently, we have applied the method to 8-channel signals (with lead I and
lead II selected from among the limb leads), and to 2-channel ones (again limb
lead I and II). Since 12-lead recordings are usually acquired in clinical environ-
ment, the latter experiment is aimed to show the proposed methods potential
180 advantages in more practical conditions.

3. Results

The spatio-temporal filter operation is illustrated in Fig. 5. We can observe
significant peaks produced by the filter within the P waves of the NSR case.
It means that at the assumed distance before the successive QRS complexes
185 (assumed PQ distance) the filter found repeatable spatio-temporal patterns,
was able to learn their shape, and started to respond to this shape with large
peaks (STP peaks in the figure). The lack of repeatable STPs in the signal of an
AF patient prevented the filter from the similar operation, and no discernible
peaks can be observed. This results in almost random positions of the detected
190 STPs for this patient.

The further stages of signal analysis are illustrated in Fig.6. For all the
assumed PQ distances, established using (8), a PQ series is determined and
for each series its standard deviation is calculated. They are presented in the
right subplots of the figure. We found significant differences between the values
195 obtained for the two classes: for NSR, smaller than 20 ms, and for AF, reaching
above 100 ms. The smallest values, finally chosen to represent the estimated

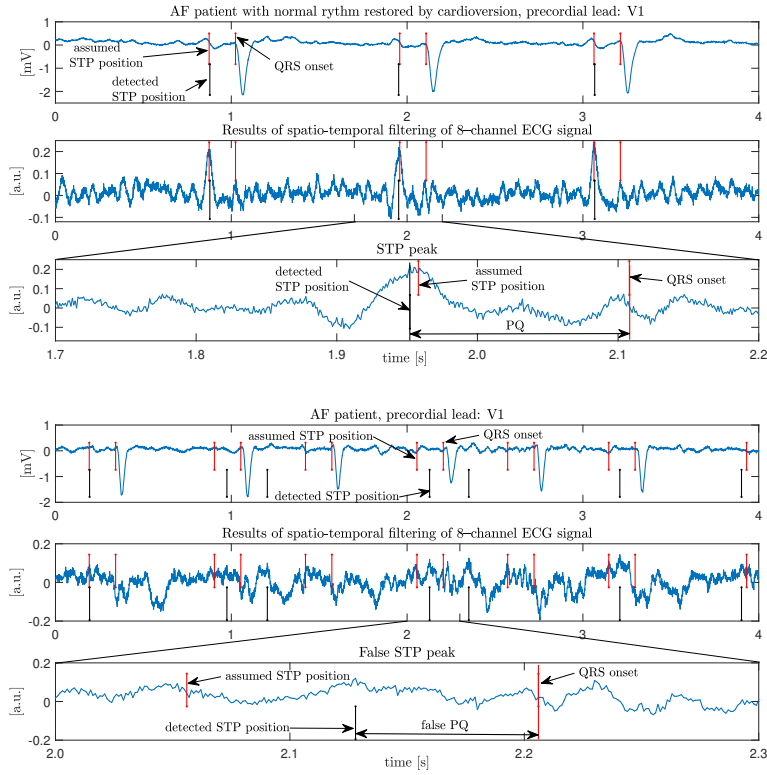


Figure 5: Illustration of the STF operation on 8-channel signals. For the normal rhythm case, significant, correctly located peaks are elicited at the output of STF (STP peaks) near the positions expected. For AF, the STF filter is not able to produce such peaks and the detected STPs are not synchronized with QRS complexes.

measure of PQ dispersion are indicated with red arrows. On the left side, we can see the corresponding PQ series: rather smooth for the NSR case and, as expected, highly unpredictable and variable for AF.

200 The analogous values, obtained for all signals considered, using all applied measures of dispersion, are presented in Fig.7. For 8-channel signals, the method proposed allows for a good discrimination between the classes considered. All the red circles except one are above the border lines plotted (whose heights were established using a simple algorithm, assuring minimal number of errors and maximal margin between the two classes) and the blue ones, below.

205

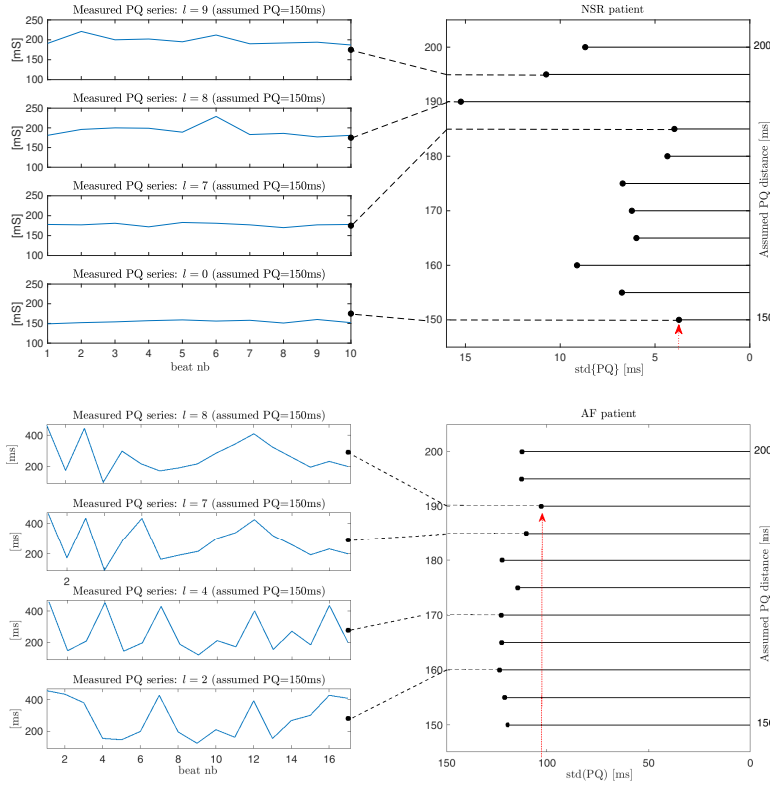


Figure 6: Results of PQ dispersion assessment for cases of normal rhythm and atrial fibrillation. On the left, we have a few selected PQ series, determined for the assumed PQ distances (positions of the magnified STPs). On the right, we can see standard deviation of the PQ series as the function of the PQ assumed. Red arrows indicate the minimal values, chosen as the final estimates of the PQ dispersion.

For most measures of dispersion, relatively wide margins exist between the NSR and the AF cases (except from the outlying one: #12). For 2-channel signals, each dispersion measure takes a wider range of values, and the NSR and AF cases are located closer. Nevertheless, even in such conditions the established border values allow for only a few classification errors for all dispersion measures applied.

The bluish segment of the figure discussed shows the indices obtained for AF patients that were successfully treated using cardioversion. For 8-channel

Table 1: Results of AF detection corresponding to Fig. 7: accuracy (ACC), number of false negatives (#FN) and number of false positives (#FP).

The length of the analysed signal excerpts						
	12 s			6 s		
Measure	ACC	#FP	#FN	ACC	#FP	#FN
8-channels signals						
STD	98.75%	0	1	97.5%	1	1
IQR	98.75%	0	1	97.5%	1	1
RNG	98.75%	0	1	96.25%	2	1
CV	98.75%	0	1	97.5%	1	1
IDS	98.75%	0	1	97.5%	1	1
MAD	98.75%	0	1	96.25%	0	3
2-channels signals						
STD	96.25%	2	1	96.25%	1	2
IQR	98.75%	0	1	93.75%	2	3
RNG	96.25%	2	1	96.25%	1	2
CV	96.25%	2	1	96.25%	1	2
IDS	96.25%	1	2	96.25%	1	2
MAD	98.75%	0	1	95%	1	3

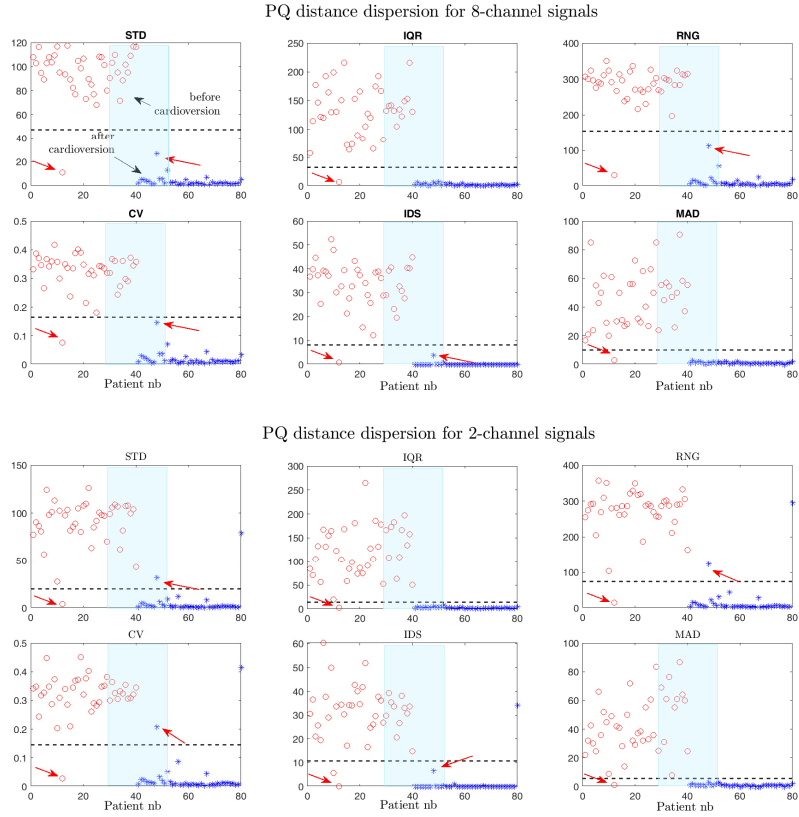


Figure 7: Plots of the calculated indices of the PQ series dispersion. The AF cases are marked with red circles and the NSR ones, with blue stars. 24 cases placed within the bluish segment: from #39 to #62, correspond to 12 AF patients who underwent cardioversion and successfully regained the sinus rhythm. Red arrows indicate two troublesome cases that led to detection errors: #12 and #48. For robust measures (IQR, MAD), the latter case disappears.

signals, all cases are correctly recognized using all the measures. For 2-channels
 215 only, three measures: IQR, IDS and MAD, have also allowed to achieve the
 goal.

The results displayed in Fig.7, have quantitatively been expressed in the left
 side of Table 1, using the number of false negatives and false positives, and the
 corresponding accuracy of AF detection (false negatives correspond to AF cases
 220 classified as NSR, and false positives vice versa).

The right side presents the analogous results obtained when the experiment was repeated using shorter signal segments. We can notice that the accuracy of classification has never fallen below 95%, irrespective of the dispersion measure, signal length and number of channels, used.

225 4. Discussion

4.1. Comparison to other methods

As we can notice in Table I, for 2-channel signals of 12 s it is more advantageous to use robust measures of dispersion (IQR and MAD), and for excerpts of 6 s, the non-robust ones (for 8-channel signals, the results are quite similar).
230 Therefore, we have selected IQR for longer and STD for shorter signal excerpts (irrespective of the channels number used). Using the AF detectors selected, we have performed an experiment according to the rules of a stratified 10-fold cross-validation. All signals have been divided in 10 groups, each containing 4 AF and 4 NSR cases. Members of each group were used as test signals while
235 the rest, as the learning ones. The experiment has been repeated 100 times with random assignment of the signals to the respective groups (preserving the same number of AF and NSR cases in each group). The results obtained are presented in Table II. For reference, we have gathered results of some other promising approaches to atrial fibrillation detection, reported in literature.

240 Many methods perform analysis of the heart rate only [4, 5, 8, 9]. Analysis of an electrocardiogram itself is proposed in [10, 13], in hybrid methods [15] or in methods based on convolutional neural networks [17, 18, 19, 20]. In [10] a spectral analysis of the P waves is performed rather for prediction than detection of paroxysmal atrial fibrillation. It is publication [13] that (like our method)
245 proposes AF detection based on the analysis of atrial activity only.

The results presented are not directly comparable because of different experiments performed and data employed. However, we can notice that our method has particularly high specificity, and accuracy comparable to the reference methods. Its disadvantage is the need to process signals of at least 2 channels. On

Table 2: Overview of different approaches (APP) to AF detection: based on heart rate (HR), atrial activity (AA) or hybrid (HR/AA) analysis, or on application of convolutional neural networks (CNN) to ECG segments. For AA and CNN approaches, we have provided the number of signal channels analysed (#CH); WL denotes the length of the analysed signal segments (windows): n.p. means not provided.

Pub.	Year	WL	# CH	APP	Se(%)	Sp(%)	Acc(%)
Zhou et al. [4]	2015	127 beats	-	HR	97.37	98.44	97.99
Islam et al. [5]	2016	70 beats	-	HR	96.39	96.38	96.38
Ebrahimzadeh et al. [8]	2018	5 min	-	HR	100	95.55	98.21
Buscema et al.[9]	2020	21 beats	-	HR	96.55	93.74	95.15
Czabanski et al. [6]	2019	21 beats	-	HR	98.94	98.39	98.66
Alcaraz et al. [10]	2015	60 min	1	AA	99.27	-	88.07
Ladavich et al. [13]	2015	7 beats	1	AA	98.09	91.66	93.12
Babaeizadeh et al. [15]	2012	n.p.	2	HR/AA	94	99	n.p.
Couceiro et al. [16]	2008	60 sec	2	HR/AA	93.80	96.09	n.p.
Purerfellner et al. [14]	2014	2 min	2	HR/AA	96	90	97.8
He et al. [17]	2018	5 beats	1	CNN	99.41	98.91	99.23
Xia et al. [18]	2018	5 sec	1	CNN	98.79	97.87	98.63
Shi et al. [19]	2020	10 sec	1	CNN	100	-	97.53
Yildirim et al. [20]	2020	10 sec	1	CNN	95.43	98.71	96.13
This study: MAD{PQ}	2021	12 sec	8	AA	100	97.90	98.95
This study: MAD{PQ}	2021	12 sec	2	AA	100	97.42	98.71
This study: STD{PQ}	2021	6 sec	8	AA	97.88	97.36	97.62
This study: STD{PQ}	2021	6 sec	2	AA	97.92	95.58	96.75

250 the other hand, it is fast, and allows to detect AF on the basis of very short
 signal intervals (similarly like the method published in [13] and as the recent
 CNN based ones). An important benefit of using this method is its good inter-
 pretability; by contrast, using CNN, we do not know what is the major reason
 of a decision chosen.

255 *4.2. Sources of AF detection errors*

Watching the upper part of Fig.7 (results for 8 channels), we can see wide
 margins between the two classes, and one red outlier in each subplot. This
 means that the method allows for very effective detection of AF, and in one case
 only, it fails completely. To see the reason, we have plotted the corresponding
 signal in Fig. 8. It appears that the signal contains exceptionally wide QRS

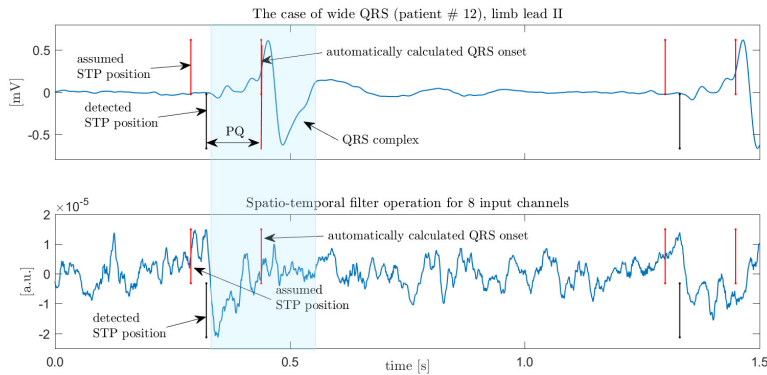


Figure 8: The case of a signal with exceptionally wide QRS complex (#12 in Fig. 7). The automatically calculated QRS onset is far from the true one, and the assumed position of the STP to be magnified is too close to this onset. Consequently, STF produces easily discernible peaks, well synchronized with the succeeding complexes. It results in the decreased PQ dispersion (see the red outlier in Fig.7)

260

complexes. Our algorithm for QRS onset detection finds the beginning of the
 most prominent wave, and in the example considered, it is necessary to find the
 smaller waves, preceding the largest one. Because of such an inadequacy of the
 algorithm, the assumed STP position is too close to the beginning part of the
 265 QRS. Consequently, the filter magnifies these parts of the respective,

and the detected peaks are well synchronized with them. It unavoidably leads to the decreased PQ dispersion, and the signal misinterpretation. In our future research, we aim to overcome this problem by replacing the applied algorithm for QRS onset localization with more advanced approach to the Q wave detection, proposed in [33].

Because of a good synchronization between the P waves and the succeeding QRS complexes (in NSR cases), it seems possible to achieve good P wave enhancement using the method of periodic component analysis [34, 35] (which was applied e.g. to the enhancement of so tiny signal components as the T wave alternans [36]). The study of this issue will also be the subject of our future research.

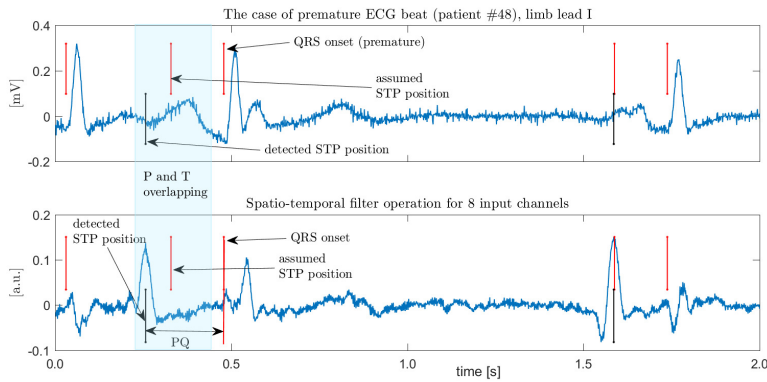


Figure 9: The case of a premature atrial contraction (PAC), with the P wave overlapping with the preceding T wave. This overlapping spoils the signal spatio-temporal structure, and prevents the STF filter from producing a peak near the position expected (assumed). However, in the case illustrated, the filter produces the peak less than 100 ms before this position. Nevertheless, even this limited error can have a damaging influence on the indices of PQ variability (see Fig. 7).

The second problematic case, indicated by a red arrow in Fig.7 corresponds to a signal that belongs to the NSR class, for which a significantly increased PQ dispersion was obtained. The signal has been presented in Fig. 9. It appears that the PQ dispersion was raised by an occurrence of a premature atrial contraction (PAC). Actually, within an interval of 12 s the signal contains

two PACs. For the corresponding beats, the PQ distance can deviate from the other values, measured. Consequently, all classical non-robust measures of PQ dispersion have discernibly been raised (see the case #48 in Fig.7). However, application of robust measures: IQR and MAD, has allowed to prevent this inconvenient phenomenon.

In table I, we can notice that, irrespective of the measure applied, for 8-channel signal of 12 s length, the case was correctly classified (for all measures $\#FP = 0$). For 2-channel signals of the same length, however, only the robust measures have allowed to achieve the goal (IQR and MAD). For 8 channels and the limited time excerpts (of 6 s) only application of MAD has allowed to prevent the false recognition of this NSR case as the AF one ($\#FP=0$), at the expense, however, of low detection sensitivity (increased number of false negatives, $\#FN=3$). Consequently, we can expect the method proposed to be able to overcome successfully the cases with limited numbers of atypical beats. This, however, depends on the dispersion measure, signal length, and number of channels, applied.

Although the method proposed has good ability to distinguish the two classes considered (what results mostly from the high performance of STF filtering), it also has an obvious limitation. If a signal processed does not contain P waves, what happens not only for atrial but also for other arrhythmias, e.g. ventricular ones, the method will recognize this, and the lack of P waves can mistakenly be considered as the AF case. We can thus conclude that at its current form, the method should not be used for discrimination between AF and all other types of cardiac rhythms. Some kind of initial classification of the signals analysed should be accomplished. Therefore, in our future experiments, we will try to precede the described analysis with application of unsupervised clustering of the ECG beats, either hierarchical [37] or based on criterion function minimization [38]. This should improve the proposed method ability to deal with different types of arrhythmias.

Considering possible applications of this method, we can begin with the most straightforward one, associated with systems for automated ECG interpretation,

at the final stage of atrial activity classification. However, the most promising one results from the most disadvantageous feature of existing systems for AF
315 detection, i.e. their low specificity. It seems that the ability to check if the P wave is present, after a system warns about possible AF, could help to reduce the number of unnecessary warnings. For both types of the systems, however, it can be particularly beneficial to exploit the proposed method ability for an early detection of AF.

320 4.3. Atrial fibrillation vs. atrial flutter

The proposed approach was specifically designed for AF detection. However, this algorithm would not work properly for the detection of macroreentrant atrial tachycardia (commonly known as atrial flutter), which could be undetected. Although both atrial arrhythmias present a continuous atrial wave
325 instead of P-waves, in the case of atrial flutter, the atrial wave is regular in shape and period, as a result of a stable macroreentrant circuit within the atria. Moreover, the ventricular activity is coupled —and therefore, synchronized— with the atrial activity. According to these features, PQ distance would exhibit low dispersion. Therefore, other features, specific to atrial flutter, should be
330 exploited to detect this atrial arrhythmia.

5. Conclusion

We introduce a concept of the PQ interval dispersion estimation for atrial fibrillation detection. Applying the noise immune method of spatio-temporal filtering to the detection of repeatable patterns within the successive P waves
335 of the multi-channel ECG signals, we are able to estimate the dispersion of the PQ interval. This index was successful for the discrimination of AF from NSR, as long as in the case of AF, P-waves are replaced by a continuous and irregular fibrillatory wave which, in addition, is no longer coupled with the ventricular rhythm.

340 The method allows for an early detection of atrial fibrillation and can advantageously be used to decrease the number of false warnings in systems based

on other features of the cardiac signals. In the experiments performed, using 8-channel and 2-channel signals, the method has allowed for almost faultless discrimination between atrial fibrillation and normal sinus rhythm.

345 6. Declaration of Competing Interest

We declare that we do not have any commercial or associative interest that represents a conflict of interest in connection with the work submitted.

7. Acknowledgments

The authors report no conflicts of interest. The authors alone are responsible
350 for the content and writing of this article. This research is partially supported by statutory funds of the Department of Cybernetics, Nanotechnology and Data Processing, Silesian University of Technology, BK-2021. Francisco Castells receives research funds from the National Research Program RETOS under grant PID2019-109547RB-I00 from the Ministry of Science, Spanish Government.

355 The work was performed using the infrastructure supported by POIG.02.03.01-24-099/13 grant: GeCONiI-Upper Silesian Center for Computational Science and Engineering.

References

- [1] W. H. Organization, Cardiovascular diseases, url-
360 <http://www.who.int/mediacentre/factsheets/fs317/en/> (2017).
- [2] H. Kamel, P. M. Okin, M. S. Elkind, C. Iadecola, Atrial fibrillation and mechanisms of stroke: time for a new model, *Stroke* 47 (3) (2016) 895–900.
- [3] L. Sörnmo, *Atrial fibrillation from an engineering perspective*, Springer, 2018.
- 365 [4] X. Zhou, H. Ding, W. Wu, Y. Zhang, A real-time atrial fibrillation detection algorithm based on the instantaneous state of heart rate, *PloS one* 10 (9) (2015) e0136544.

- 370 [5] M. S. Islam, N. Ammour, N. Alajlan, H. Aboalsamh, Rhythm-based heart-beat duration normalization for atrial fibrillation detection, *Computers in biology and medicine* 72 (2016) 160–169.
- [6] R. Czabanski, K. Horoba, J. Wrobel, A. Matonia, R. Martinek, T. Kupka, M. Jezewski, R. Kahankova, J. Jezewski, J. M. Leski, Detection of atrial fibrillation episodes in long-term heart rhythm signals using a support vector machine, *Sensors* 20 (3) (2020) 765.
- 375 [7] A. M. Climent, M. de la Salud Guillem, D. Husser, F. Castells, J. Millet, A. Bollmann, Poincaré surface profiles of rr intervals: A novel noninvasive method for the evaluation of preferential av nodal conduction during atrial fibrillation, *IEEE Transactions on Biomedical Engineering* 56 (2) (2009) 433–442. doi:10.1109/TBME.2008.2003273.
- 380 [8] E. Ebrahimzadeh, M. Kalantari, M. Joulani, R. S. Shahraki, F. Fayaz, F. Ahmadi, Prediction of paroxysmal atrial fibrillation: A machine learning based approach using combined feature vector and mixture of expert classification on hrv signal, *Computer methods and programs in biomedicine* 165 (2018) 53–67.
- 385 [9] P. M. Buscema, E. Grossi, G. Massini, M. Breda, F. Della Torre, Computer aided diagnosis for atrial fibrillation based on new artificial adaptive systems, *Computer Methods and Programs in Biomedicine* 191 (2020) 105401.
- [10] R. Alcaraz, A. Martínez, J. J. Rieta, Role of the p-wave high frequency energy and duration as noninvasive cardiovascular predictors of paroxysmal atrial fibrillation, *Computer Methods and Programs in Biomedicine* 119 (2) 390 (2015) 110–119.
- [11] M. Stridh, L. Sörnmo, Spatiotemporal QRST cancellation techniques for analysis of atrial fibrillation, *IEEE Transactions on Biomedical Engineering* 48 (2001) 105–111.

- 395 [12] F. Castells, J. J. Rieta, J. Millet, V. Zarzoso, Spatiotemporal blind source separation approach to atrial activity estimation in atrial tachyarrhythmias, *IEEE Transactions on Biomedical Engineering* 52 (2) (2005) 258–267.
- [13] S. Ladavich, B. Ghoraani, Rate-independent detection of atrial fibrillation by statistical modeling of atrial activity, *Biomedical Signal Processing and Control* 18 (2015) 274–281.
- 400 [14] H. Pürerfellner, E. Pokushalov, S. Sarkar, J. Koehler, R. Zhou, L. Urban, G. Hindricks, P-wave evidence as a method for improving algorithm to detect atrial fibrillation in insertable cardiac monitors, *Heart Rhythm* 11 (9) (2014) 1575–1583.
- 405 [15] S. Babaeizadeh, R. E. Gregg, E. D. Helfenbein, J. M. Lindauer, S. H. Zhou, Improvements in atrial fibrillation detection for real-time monitoring, *Journal of electrocardiology* 42 (6) (2009) 522–526.
- [16] R. Couceiro, P. Carvalho, J. Henriques, M. Antunes, M. Harris, J. Habetha, Detection of atrial fibrillation using model-based ecg analysis (2008) 1–5.
- 410 [17] R. He, K. Wang, N. Zhao, Y. Liu, Y. Yuan, Q. Li, H. Zhang, Automatic detection of atrial fibrillation based on continuous wavelet transform and 2d convolutional neural networks, *Frontiers in physiology* 9 (2018) 1206.
- [18] Y. Xia, N. Wulan, K. Wang, H. Zhang, Detecting atrial fibrillation by deep convolutional neural networks, *Computers in biology and medicine* 93 (2018) 84–92.
- 415 [19] H. Shi, H. Wang, C. Qin, L. Zhao, C. Liu, An incremental learning system for atrial fibrillation detection based on transfer learning and active learning, *Computer Methods and Programs in Biomedicine* 187 (2020) 105219.
- [20] O. Yildirim, M. Talo, E. J. Ciaccio, R. San Tan, U. R. Acharya, Accurate deep neural network model to detect cardiac arrhythmia on more than 10,000 individual subject ecg records, *Computer methods and programs in biomedicine* 197 (2020) 105740.
- 420

- [21] N. R. Jones, C. J. Taylor, F. D. R. Hobbs, L. Bowman, B. Casadei, Screening for atrial fibrillation: a call for evidence, *European Heart Journal* 41 (10) (2019) 1075–1085. `arXiv:https://academic.oup.com/eurheartj/article-pdf/41/10/1075/32816847/ehz834.pdf`, doi: 10.1093/eurheartj/ehz834.
URL `https://doi.org/10.1093/eurheartj/ehz834`
- [22] J. Mandrola, A. Foy, Downsides of detecting atrial fibrillation in asymptomatic patients, *American family physician* 99 (2019) 354–355.
- [23] M. Kotas, J. Jezewski, K. Horoba, A. Matonia, Application of spatio-temporal filtering to fetal electrocardiogram enhancement, *Computer methods and programs in biomedicine* 104 (1) (2011) 1–9.
- [24] F. Castells, Blind source separation with prior source knowledge for the analysis of atrial tachyarrhythmias. signal modelling, estimation and validation, Ph.D. thesis, Universitat Politècnica de València, Spain (2003).
- [25] A. Goldberger, L. Amaral, L. Glass, J. Hausdorff, P. Ivanov, R. Mark, J. Mietus, G. Moody, C. Peng, H. Stanley, Physiobank, physiotoolkit, and physionet: components of a new research resource for complex physiologic signals, *Circulation* 101 (2000) e215–e220.
- [26] S. M. Kay, *Fundamentals of statistical signal processing*, Prentice Hall PTR, 1993.
- [27] B. Yang, H. Li, Q. Wang, Y. Zhang, Subject-based feature extraction by using fisher wpd-csp in brain–computer interfaces, *Computer Methods and Programs in Biomedicine* 129 (2016) 21–28.
- [28] A. Miladinović, M. Ajčević, J. Jarmolowska, U. Marusic, M. Colussi, G. Silveri, P. P. Battaglini, A. Accardo, Effect of power feature covariance shift on bci spatial-filtering techniques: A comparative study, *Computer Methods and Programs in Biomedicine* 198 (2020) 105808.

- 450 [29] J. Pan, W. J. Tompkins, A real-time qrs detection algorithm, *IEEE transactions on biomedical engineering* (3) (1985) 230–236.
- [30] H. Azami, K. Mohammadi, B. Bozorgtabar, An improved signal segmentation using moving average and savitzky-golay filter (2012).
- [31] N. Miljković, N. Popović, O. Djordjević, L. Konstantinović, T. B. Šekara,
455 Ecg artifact cancellation in surface emg signals by fractional order calculus application, *Computer methods and programs in biomedicine* 140 (2017) 259–264.
- [32] C. Croarkin, P. Tobias, J. Filliben, B. Hembree, W. Guthrie, et al.,
460 Nist/sematech e-handbook of statistical methods, NIST/SEMATECH, July. Available online: <http://www.itl.nist.gov/div898/handbook> (2006).
- [33] J. P. Martínez, R. Almeida, S. Olmos, A. P. Rocha, P. Laguna, A wavelet-based ecg delineator: evaluation on standard databases, *IEEE Transactions on biomedical engineering* 51 (4) (2004) 570–581.
- [34] L. K. Saul, J. B. Allen, Periodic component analysis: an eigenvalue method
465 for representing periodic structure in speech, in: *Nips*, 2000, pp. 807–813.
- [35] R. Sameni, C. Jutten, M. B. Shamsollahi, Multichannel electrocardiogram decomposition using periodic component analysis, *IEEE transactions on biomedical engineering* 55 (8) (2008) 1935–1940.
- [36] V. Monasterio, G. D. Clifford, P. Laguna, J. P. MARTInez, A multilead
470 scheme based on periodic component analysis for t-wave alternans analysis in the ecg, *Annals of biomedical engineering* 38 (8) (2010) 2532–2541.
- [37] J. M. Leski, M. Kotas, Hierarchical clustering with planar segments as prototypes, *Pattern Recognition Letters* 54 (2015) 1–10.
- [38] J. M. Leski, M. Kotas, On robust fuzzy c-regression models, *Fuzzy Sets and Systems* 279 (2015) 112–129.
475